A Gaussian-2 and Gaussian-3 Study of Alkoxide Anion Decompositions. 2. Alkane Eliminations of $(CH_3)_2(C_2H_5)CO^-$ and $(i\text{-}Pr)(C_2H_5)_2CO^-$

Justin Kai-Chi Lau and Wai-Kee Li*

Department of Chemistry, The Chinese University of Hong Kong, Shatin, N.T., Hong Kong

S.-W. Chiu*

Department of Molecular and Integrative Physiology and Beckman Institute for Advanced Studies, University of Illinois, 405 N. Mathews, Urbana, Illinois 61801

Received: August 25, 2001; In Final Form: October 8, 2001

The energetics and decomposition mechanisms of $(CH_3)_2(C_2H_5)CO^-$ and $(i\text{-}Pr)(C_2H_5)_2CO^-$ have been studied at the G2++, G3, and G3(MP2) levels of theory. It is found that the energies required for methane elimination of $(CH_3)_2(C_2H_5)CO^-$ are less than that for ethane elimination, in agreement with experiment that only the former reaction is observed. On the other hand, the energies required for ethane and propane eliminations of $(i\text{-}Pr)(C_2H_5)_2CO^-$ are within 2 kJ mol^{-1} of each other. So both eliminations are likely, as observed experimentally. Mechanistically, it is found that alkane dissociation of the tertiary alkoxide anions follows a pathway similar to that of methane elimination for primary and secondary alkoxides. The dissociation starts with detachment of a carbanion, followed by proton abstraction to form an alkane molecule, with an ion−molecular complex being formed as an intermediate.

Introduction

The decomposition of alkoxide anions has been studied fairly extensively both experimentally[1−9] and theoretically.[10−12] The dissociation mechanism of simple alkoxide anions has been investigated by collision-activated dissociation (CAD) which showed that the elimination of alkoxide anions should proceed via a stepwise pathway.[1−7] Besides, the technique of infrared multiple photon (IRMP) photodissociation has also been applied to study these dissociations.[8,9] Brauman and co-workers further suggested that the initial bond breaking involved in the dissociation of alkoxide anions should be heterolytic rather than homolytic.[8] On the other hand, different levels of theory have also been employed to study the energetics and mechanisms on the hydrogen and methane eliminations of alkoxide anions.[10−12] Bowie et al.[10,11] have studied the mechanism of the elimination reaction of ethoxide and *tert*-butoxide anions. Also, we have recently reported[12] the energy barriers and reaction mechanisms of hydrogen and methane elimination of several simple alkoxide anions at the G2++[13] and G3[14] levels of theory. All of these findings are consistent with the results reported from experiments. However, it appears that there is a lack of theoretical study on the methane, ethane, and propane eliminations from tertiary alkoxide anions, and this is the subject we take up in this work.

Here we study the following alkane eliminations of tertiary alkoxide anions $(CH_3)_2(C_2H_5)CO^-$ and $(i\text{-}Pr)(C_2H_5)_2CO^-$ at a high theoretical level:

$$(CH_3)_2(C_2H_5)CO^- \rightarrow CH_3CH{=}C(CH_3)O^- + CH_4 \qquad (1a)$$

$$(CH_3)_2(C_2H_5)CO^- \rightarrow CH_2{=}C(C_2H_5)O^- + CH_4 \qquad (1b)$$

$$(CH_3)_2(C_2H_5)CO^- \rightarrow CH_2{=}C(CH_3)O^- + C_2H_6 \qquad (1c)$$

$$(i\text{-}Pr)(C_2H_5)_2CO^- \rightarrow CH_3CH{=}C(C_2H_5)O^- + C_3H_8 \qquad (2a)$$

$$(i\text{-}Pr)(C_2H_5)_2CO^- \rightarrow (CH_3)_2C{=}C(C_2H_5)O^- + C_2H_6 \qquad (2b)$$

$$(i\text{-}Pr)(C_2H_5)_2CO^- \rightarrow CH_3CH{=}C(i\text{-}Pr)O^- + C_2H_6 \qquad (2c)$$

This study attempts to answer some of the questions raised in our previous paper[12] regarding alkoxide anion dissociations: (1) When the anions are tertiary alkoxides, do their dissociations proceed via a stepwise or a concerted mechanism? (2) Why is the heterolytic cleavage more favorable than the homolytic one, as deduced from experimental results? Also, we will attempt to draw a conclusion on the dissociation mechanisms of primary, secondary, and tertiary alkoxide anions.

Methods of Calculations

All of the calculations were carried out on DEC 500au, XP900, XP1000, as well as on an SGI Origin 2000 High-Performance Server, using the Gaussian 94[15] and Gaussian 98[16] packages of programs. The computational models we employed for $(CH_3)_2(C_2H_5)CO^-$ were the modified Gaussian-2 (G2++) and Gaussian-3 (G3) levels of theory. The details of these theoretical models have been described in our previous work.[12]

---

* To whom correspondence should be addressed.

10.1021/jp013295r CCC: $20.00

TABLE 1: Heterolytic and Homolytic Bond Dissociation Energies of Various Alkoxide Anions at the G3 Level[a,b]

$(C_2H_5)(CH_3)C{=}O + CH_3^-$	←	$(CH_3)_2(C_2H_5)CO^-$ (**1**)	→	$(C_2H_5)(CH_3)C{=}O^- + {}^{\bullet}CH_3$
200.4		0		287.2
$(CH_3)_2C{=}O + C_2H_5^-$	←	$(CH_3)_2(C_2H_5)CO^-$ (**1**)	→	$(CH_3)_2C{=}O^- + {}^{\bullet}C_2H_5$
224.3		0		296.0
$(i\text{-Pr})(C_2H_5)C{=}O + C_2H_5^-$	←	$(i\text{-Pr})(C_2H_5)_2CO^-$ (**7**)	→	$(i\text{-Pr})(C_2H_5)C{=}O^- + {}^{\bullet}C_2H_5$
209.5		0		264.1
$(C_2H_5)_2C{=}O + i\text{-Pr}^-$	←	$(i\text{-Pr})(C_2H_5)_2CO^-$ (**7**)	→	$(C_2H_5)_2C{=}O^- + {}^{\bullet}i\text{-Pr}$
197.8		0		263.4

[a] The species shown in the first column are the products of a heterolytic cleavage of the alkoxide anions given in the middle column; those given in the last column are the products of a homolytic cleavage. [b] The values for **7** and all of the related species are calculated at the G3(MP2) level.

Because of the large size of the $(i\text{-Pr})(C_2H_5)_2CO^-$ system, a less expensive variant of the G3 method, G3(MP2),[17] was employed for all of the stable and transition structures involved in the dissociation reactions. In the G3(MP2) model, structures are optimized at the MP2(Full)/6-31G(d) level and single-point calculations at the QCISD(T)/6-31G(d) and MP2/G3MP2large levels are carried out. Here G3MP2large is a basis set specially designed for the G3(MP2) model. Furthermore, higher level correction is also included to give the E_e of the system. The MP2(Full)/6-31G(d) harmonic vibrational frequencies, scaled by 0.9661, are used for the zero-point vibration energy (ZPVE) correction at 0 K ($E_0 = E_e + \text{ZPVE}$).

Before proceeding further, some remarks are made regarding the three chosen methods. It is noted that the G2++ model was specifically designed for anionic systems (recalling that G2 does not treat hydride anion satisfactorily),[13] and the G2++ results obtained so far are quite good.[12,13] On the other hand, the G3 model is the latest version of the Gaussian-*n* methods, and the present application may serve as a benchmark on how well this model does in treating anionic systems. Finally, for systems that are too large to be treated by either G2++ or G3, the less expensive G3(MP2) method is used instead.

The thermochemical data for ions presented in this work are based on the ion convention (frozen electron).[18] The G2++, G3, or G3(MP2) heats of formation at temperature T (ΔH^o_{fT}) for anion AB^- reported in this work were calculated from the corresponding heats of reaction $\Delta H^o_{rT}(AB^- \rightarrow A + B + e^-)$ and the experimental $\Delta H^o_{fT}(A)$ and $\Delta H^o_{fT}(B)$ for elements A and B, respectively, with $\Delta H^o_{fT}(e^-) = 0$. This method has been described in more detail in our previous work.[19]

In this work, many transition structures (TSs) were located. The initial structure of each TS may be obtained by scanning along an approximate reaction coordinate. The "reactant(s)" and "product(s)" of each TS were confirmed by intrinsic reaction coordinate calculations.

Results and Discussion

The heterolytic and homolytic bond dissociation energies of the alkoxide anions $(CH_3)_2(C_2H_5)CO^-$ (**1**) and $(i\text{-Pr})(C_2H_5)_2CO^-$ (**7**) are summarized in Table 1. The G2++ and G3 standard heats of formation for the species involved in reactions 1a, 1b, and 1c at 0 and 298 K are listed in Table 2, whereas the G3(MP2) results for the species involved in reactions 2a, 2b, and 2c are given in Table 3. Also, the energy profiles for these six dissociation reactions are displayed in Figures 1 and 2. The geometries for all of the stable and transition structures are illustrated in Figure 3. Throughout this work, G2++ and G3MP2 energies are used in discussions unless explicitly stated otherwise.

TABLE 2: G2++ and G3 Total Energies[a] (E_0), Enthalpies (H_{298}), and Standard Heats of Formation at 0 K (ΔH^o_{f0}) and 298 K (ΔH^o_{f298}) of the Species Involved in the Fragmentation Reaction of $(CH_3)_2(C_2H_5)CO^-$ (1)

species	E_0 (hartree)	H_{298} (hartree)	ΔH^o_{f0} (kJ mol^{-1})	ΔH^o_{f298} (kJ mol^{-1})
1	**−271.86028**	**−271.85153**	**−267.9**	**−298.3**
	−272.13111	*−272.12251*	*−255.0*	*−285.9*
				(−300 ± 13)[b]
				(−300 ± 8.8)[c]
2	**−271.80964**	**−271.79810**	**−134.9**	**−158.0**
	−272.08140	*−272.06997*	*−124.5*	*−148.0*
(**3a** + **3b**)[d]	**−271.86296**	**−271.85155**		
	−272.13394	*−272.12288*		
(**4a** + **4b**)[d]	**−271.86325**	**−271.85233**		
	−272.13418	*−272.12345*		
5	**−271.80172**	**−271.79083**	**−114.1**	**−139.0**
	−272.07025	*−272.05961*	*−95.3*	*−120.8*
(**6a** + **6b**)[d]	**−271.85653**	**−271.84608**		
	−272.12743	*−272.11725*		
TS(**1**→**2**)	**−271.80523**	**−271.79423**	**−123.3**	**−147.9**
	−272.07684	*−272.06594*	*−112.6*	*−137.4*
TS(**2**→**3**)	**−271.81082**	**−271.79976**	**−138.0**	**−162.4**
	−272.08309	*−272.07213*	*−129.0*	*−153.6*
TS(**2**→**4**)	**−271.80999**	**−271.79922**	**−135.8**	**−161.0**
	−272.08229	*−272.07162*	*−126.9*	*−152.3*
TS(**1**→**5**)	**−271.79507**	**−271.78446**	**−96.6**	**−122.2**
	−272.06365	*−272.05326*	*−77.9*	*−104.1*
TS(**5**→**6**)	**−271.80230**	**−271.79212**	**−115.6**	**−142.3**
	−272.07082	*−272.06105*	*−96.7*	*−124.5*

[a] G2++ energies are shown in bold font, and G3 energies are in italic font. [b] The experimental value, taken from ref 18, is given in brackets. [c] The experimental value, taken from ref 21, is given in brackets. [d] Here, the two fragments are assumed to be infinitely apart.

TABLE 3: G3(MP2) Total Energies (E_0), Enthalpies (H_{298}), and Standard Heats of Formation at 0 K (ΔH^o_{f0}) and 298 K (ΔH^o_{f298}) of the Species Involved in the Fragmentation Reaction of $(i\text{-Pr})(C_2H_5)_2CO^-$ (6)

species	E_0 (hartree)	H_{298} (hartree)	ΔH^o_{f0} (kJ mol^{-1})	ΔH^o_{f298} (kJ mol^{-1})
7	−389.60248	−389.58989	−281.1	−328.7
8	−389.55188	−389.53710	−148.2	−190.1
(**9a** + **9b**)[a]	−389.60502	−389.59111		
10	−389.55481	−389.53964	−155.9	−196.8
(**11a** + **11b**)[a]	−389.60424	−389.58983		
(**12a** + **12b**)[a]	−389.61013	−389.59594		
TS(**7**→**8**)	−389.54730	−389.53318	−136.2	−179.9
TS(**8**→**9**)	−389.55099	−389.53714	−145.9	−190.2
TS(**7**→**10**)	−389.54633	−389.53205	−133.7	−176.9
TS(**10**→**11**)	−389.55667	−389.54247	−160.8	−204.2
TS(**10**→**12**)	−389.54916	−389.53494	−141.1	−184.5

[a] Here the two fragments are assumed to be infinitely apart.

Initial Bond Cleavage of Alkoxide Anions. As mentioned in our previous paper,[12] the dissociation of alkoxide anions is mediated by ion−neutral complexes (INCs). We can determine whether the reaction is dominated by ion−molecular complexes (IMCs) or ion−radical complexes (IRCs) when we compare the energetics for the heterolytic and homolytic pathways. From Table 1, it is seen that all of the heterolytic cleavages require less energie than their homolytic counterparts. So, we can simply conclude that, for alkoxide anion dissociations, the heterolytic

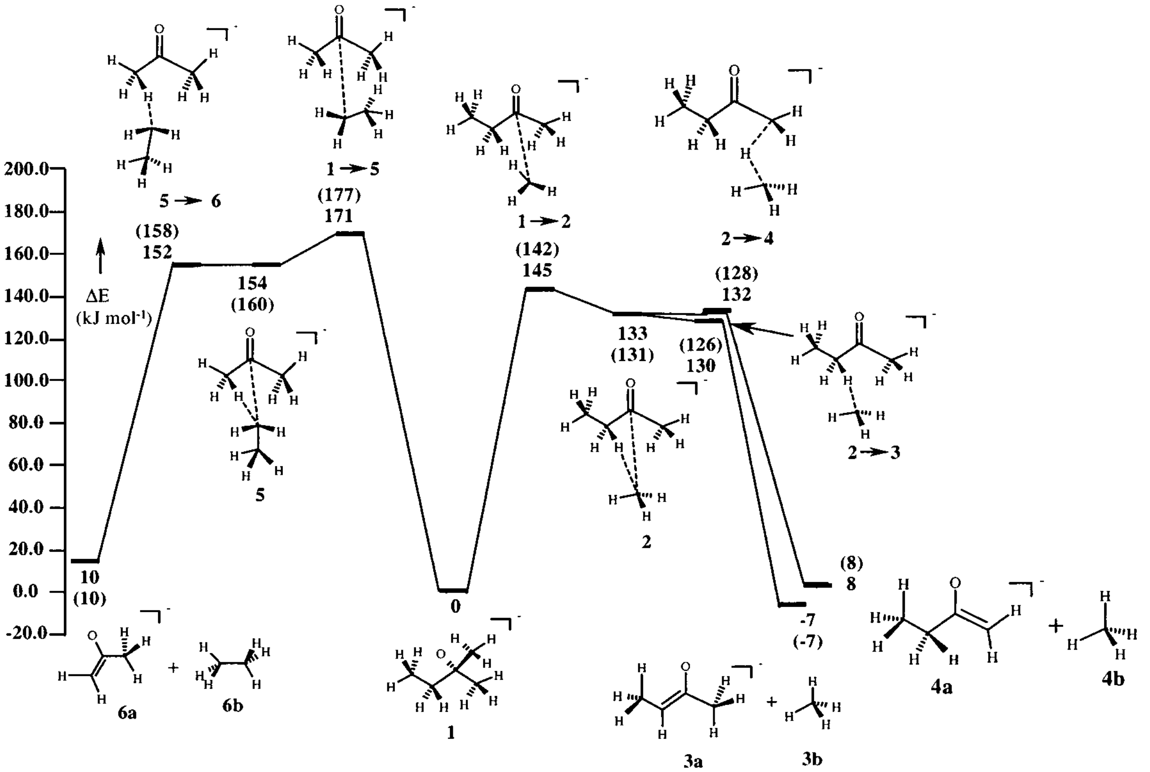

Figure 1. G2++ energy profiles of the dissociations for $(CH_3)_2(C_2H_5)CO^-$ (**1**). The G3 relative energies are given in parentheses.

bond cleavage is more favorable than the homolytic one. In other words, the reaction starts with heterolytic bond cleavage to form the carbanion rather than homolytic bond cleavage to form the alkyl radical. Based on these results, we infer that the INCs involved in the dissociations studied in this work are IMCs rather than IRCs. These results are consistent with our previous study. In the homolytic bond cleavage process, two open-shell species, i.e., radicals, are formed, whereas the heterolytic cleavage forms two close-shell species. It is generally held that close-shell species should be more stable than the open-shell ones. So, it is not surprising that the heterolytic cleavage is more favorable than the homolytic one in the dissociation of an alkoxide anion.

Dissociation of Alkoxide Anions. *Dissociation of* $(CH_3)_2(C_2H_5)CO^-$ *(1).* As shown in Figure 1, there are three possible dissociations for **1**: two different eliminations of methane and the elimination of ethane. These reactions may be described as

$$(CH_3)_2(C_2H_5)CO^- \ (\mathbf{1}) \rightarrow TS(\mathbf{1} \rightarrow \mathbf{2}) \rightarrow [H_3C^- \cdots (CH_3)(C_2H_5)CO] \ (\mathbf{2}) \rightarrow TS(\mathbf{2} \rightarrow \mathbf{3}) \rightarrow CH_3CH{=}C(CH_3)O^- \ (\mathbf{3a}) + CH_4 \ (\mathbf{3b}) \quad (1a)$$

$$(CH_3)_2(C_2H_5)CO^- \ (\mathbf{1}) \rightarrow TS(\mathbf{1} \rightarrow \mathbf{2}) \rightarrow [H_3C^- \cdots (CH_3)(C_2H_5)CO] \ (\mathbf{2}) \rightarrow TS(\mathbf{2} \rightarrow \mathbf{4}) \rightarrow CH_2{=}C(C_2H_5)O^- \ (\mathbf{4a}) + CH_4 \ (\mathbf{4b}) \quad (1b)$$

$$(CH_3)_2(C_2H_5)CO^- \ (\mathbf{1}) \rightarrow TS(\mathbf{1} \rightarrow \mathbf{5}) \rightarrow [H_5C_2^- \cdots (CH_3)_2CO] \ (\mathbf{5}) \rightarrow TS(\mathbf{5} \rightarrow \mathbf{6}) \rightarrow CH_2{=}C(CH_3)O^- \ (\mathbf{6a}) + C_2H_6 \ (\mathbf{6b}) \quad (1c)$$

It is noted that, in the G3 calculations of reactions 1a and 1b, the structures of TS(**1** → **2**), **2**, TS(**2** → **3**), and TS(**2** → **4**) were optimized at the MP2(Full)/6-31++G(d) level because **2**, TS(**2** → **3**), and TS(**2** → **4**) could not be located at the MP2(Full)/6-31G(d) level. It is known that the use of diffuse functions is very important in the geometry optimization and energy calculations for the anions. Although **1** is a tertiary alkoxide anion, it is still possible for it to undergo hydrogen elimination via IMC $[H^- \cdots c\text{-}CH_2C(C_2H_5)(CH_3)O]$, i.e., **1** → $[H^- \cdots c\text{-}CH_2C(C_2H_5)(CH_3)O] \rightarrow H_2 + C_5H_9O^-$ $[c\text{-}CHC(C_2H_5)(CH_3)O^-$ or $(C_2H_5)(CH_3)C{=}CHO^-]$. However, as we discussed in our previous paper,[12] this kind of reaction is energetically noncompetitive to alkane eliminations. From Figure 1, it is seen that the elimination of methane starts with methyl anion dissociation, followed by proton abstraction (from two different sources) to form the methane molecule. On the other hand, the elimination of ethane starts with ethyl anion dissociation, followed by proton abstraction to form the ethane molecule. All of these pathways involve the formation of IMC intermediates. In other words, the dissociations follow a stepwise mechanism.

From the G2++ potential energy curves for reactions 1a–c shown in Figure 1, the overall barrier for either of the two CH_4 eliminations is 145 kJ mol^{-1}, whereas that for the elimination of ethane is 171 kJ mol^{-1}. In other words, the eliminations of methane are more favorable by 26 kJ mol^{-1} (the G3 results are similar). This is consistent with the results reported by Brauman and co-workers,[8] where only methane was observed in their experiments. The G2++ (or G3) results are also in line with the low-energy CAD study[1] of **1**: methane elimination is the dominant channel observed among its dissociation pathways, and elimination of ethane from **1** increases as collision energy increases.[1]

The energy barriers of reactions 1a and 1b are the same (145 kJ mol^{-1}). However, fragment **3a** is more stable than **4a** by 15 kJ mol^{-1}. Hence, reaction 1a is thermodynamically more favorable than reaction 1b. In other words, among the three dissociation pathways of **1**, the elimination of methane leading to the formation of **3a** and **3b** is the most favorable.

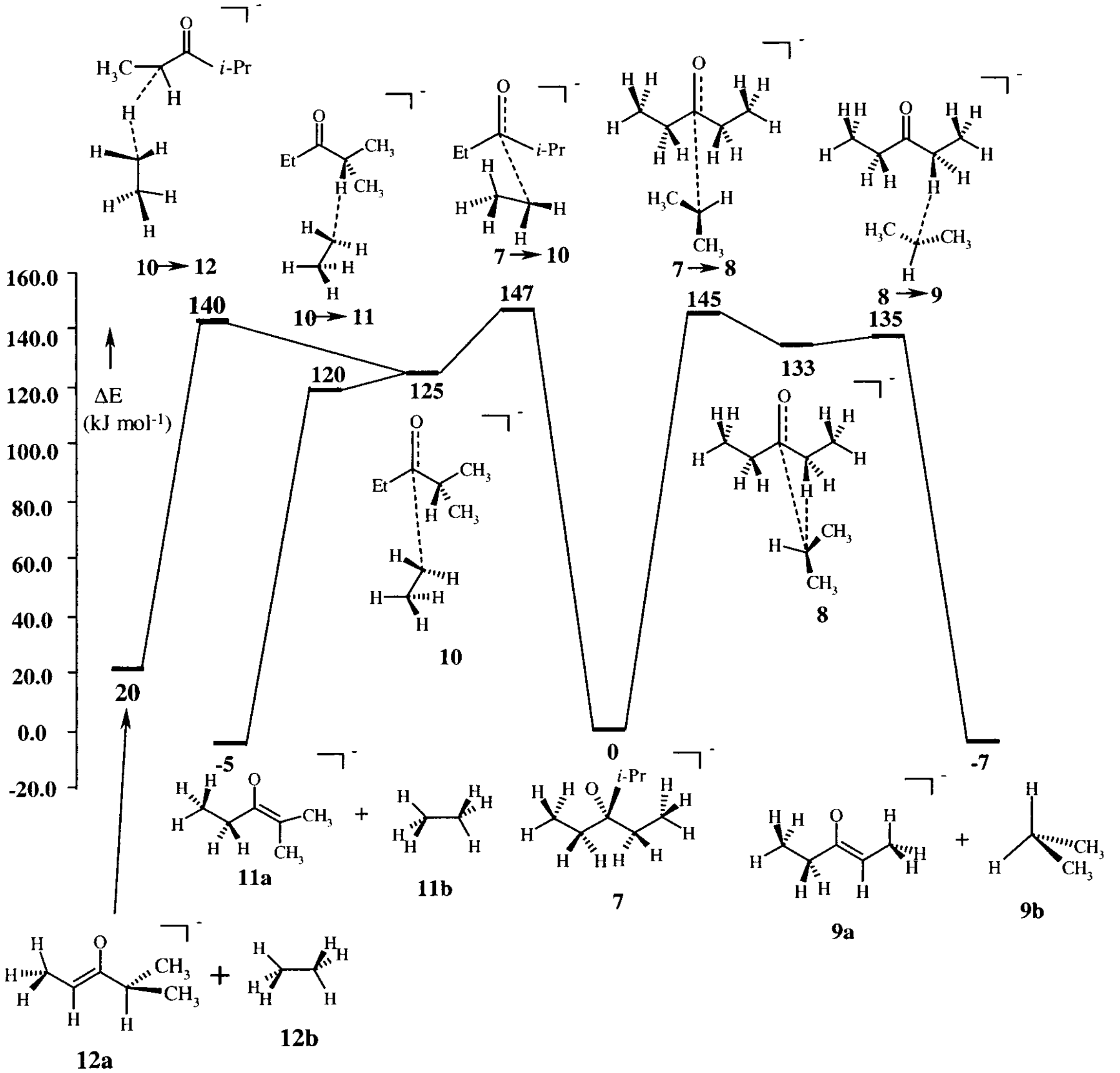

Figure 2. G3(MP2) energy profiles of the dissociations for $(i\text{-Pr})(C_2H_5)_2CO^-$ (**6**).

Dissociation of (i-Pr)(C₂H₅)₂CO⁻ (7). There are also three dissociations to be studied, two eliminations of ethane and one elimination of propane, as shown in Figure 2:

$$(i\text{-Pr})(C_2H_5)_2CO^- \ (\mathbf{7}) \rightarrow \mathrm{TS}(\mathbf{7} \rightarrow \mathbf{8}) \rightarrow [(CH_3)_2HC^- \cdots (C_2H_5)_2CO] \ (\mathbf{8}) \rightarrow \mathrm{TS}(\mathbf{8} \rightarrow \mathbf{9}) \rightarrow CH_3CH{=}C(C_2H_5)O^- \ (\mathbf{9a}) + C_3H_8 \ (\mathbf{9b}) \quad (2a)$$

$$(i\text{-Pr})(C_2H_5)_2CO^- \ (\mathbf{7}) \rightarrow \mathrm{TS}(\mathbf{7} \rightarrow \mathbf{10}) \rightarrow [H_5C_2^- \cdots (i\text{-Pr})(C_2H_5)CO] \ (\mathbf{10}) \rightarrow \mathrm{TS}(\mathbf{10} \rightarrow \mathbf{11}) \rightarrow (CH_3)_2C{=}C(C_2H_5)O^- \ (\mathbf{11a}) + C_2H_6 \ (\mathbf{11b}) \quad (2b)$$

$$(i\text{-Pr})(C_2H_5)_2CO^- \ (\mathbf{7}) \rightarrow \mathrm{TS}(\mathbf{7} \rightarrow \mathbf{10}) \rightarrow [H_5C_2^- \cdots (i\text{-Pr})(C_2H_5)CO] \ (\mathbf{10}) \rightarrow \mathrm{TS}(\mathbf{10} \rightarrow \mathbf{12}) \rightarrow CH_3CH{=}C(i\text{-Pr})O^- \ (\mathbf{12a}) + C_2H_6 \ (\mathbf{12b}) \quad (2c)$$

The dissociation mechanisms for **7** are very similar to those of **1**: elimination of ethane starts with ethyl anion elimination, followed by proton abstraction on the neighboring isopropyl or ethyl group. On the other hand, the elimination of propane starts with propyl anion elimination, followed by proton abstraction on the neighboring ethyl group. All reactions involve the formation of IMC intermediates. From Figure 2, the G3(MP2) potential energy curve shows that the energy barrier for the elimination of ethane is 147 kJ mol^{-1}, whereas the barrier for the elimination of propane is 145 kJ mol^{-1}. The small difference in the energy barriers suggests that both the ethane and propane eliminations of **7** are equally likely. Again, this conclusion is consistent with the results obtained by Brauman et al.,[8] which indicate that almost equal amounts of ethane (45%) and propane (55%) are detected as products in the dissociation of **7**. It is noted that the TS(**10** → **12**) involved in reaction 2c was optimized at the HF/6-31+G(d) level. We tried to locate it at a higher level, but without success.

General Dissociation Mechanism of Alkoxide Anions. In the previous work[12] and the present one, the dissociations of six alkoxide anions—CH_3O^-, $CH_3CH_2O^-$, $(CH_3)_2CHO^-$, $(CH_3)_3CO^-$, $(CH_3)_2(C_2H_5)CO^-$, and $(i\text{-Pr})(C_2H_5)_2CO^-$—have been studied at the G2++, G3, and G3(MP2) levels of theory. On the basis of the calculated results, it is found that the mechanisms of hydrogen and alkane eliminations are very similar. They proceed through stepwise pathways, and the initial bond cleavage should be heterolytic rather than homolytic; that is, hydride ions or carbanions are first formed in the dissociations. For the hydrogen elimination from an alkoxide anion, the reaction starts with hydride ion dissociation. Then an IMC

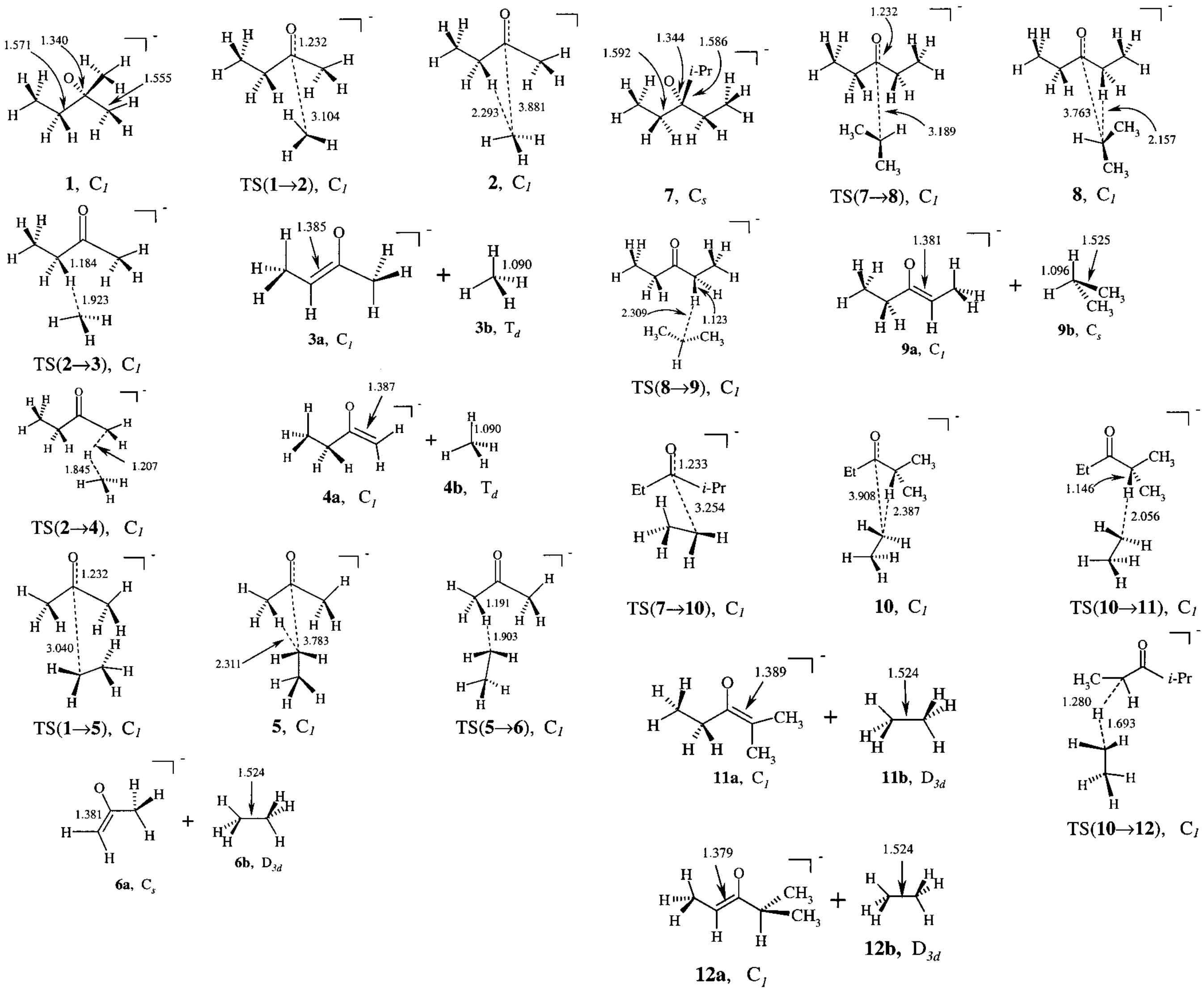

Figure 3. Optimized structures of all of the species involved in the fragmentation reactions of $(CH_3)_2(C_2H_5)CO^-$ (**1**) and $(i\text{-Pr})(C_2H_5)_2CO^-$ (**7**). All of the structures involved with the reactions of **1** were optimized at the MP2(Full)/6-31++G(d) level. Those involved with the reactions of **7** were determined at the MP2(Full)/6-31G(d) level.

intermediate is formed. Finally, this intermediate abstracts a proton to form a hydrogen molecule. On the other hand, alkane eliminations start with alkyl anion dissociation, followed by formation of an IMC intermediate. This intermediate then abstracts a proton to form an alkane molecule. In other words, the mechanisms for methane, ethane, and propane eliminations are very similar. It is noted that the charged (hydride ions or alkyl anions) and neutral fragments are held together by electrostatic interaction, and the fragments sojourn in the vicinity of one another long enough to undergo a subsequent ion−neutral reaction.[20]

Conclusions

In this work dissociation mechanisms of $(CH_3)_2(C_2H_5)CO^-$ (**1**) and $(i\text{-Pr})(C_2H_5)_2CO^-$ (**7**) have been studied using the G2++, G3, and G3(MP2) levels of theory. On the basis of our calculated results, we find that methane elimination is more favorable than ethane elimination for **1**. On the other hand, both ethane and propane eliminations are equally likely for **7**. The dissociations of alkoxide anions proceed through a stepwise pathway, and the initial bond breaking should be heterolytic rather than homolytic. The alkane elimination starts with alkyl anion elimination, followed by proton abstraction to form the alkane molecule. In addition, an IMC intermediate is also involved.

Acknowledgment. J.K.C.L. and W.K.L. are grateful to the Computer Services Centre of The Chinese University of Hong Kong for its generous allocation of computer time on the SGI Origin 2000 High-Performance Server. The work described in this paper was supported by a grant from the Research Grants Council of the Hong Kong Special Administrative Region (Project No. CUHK4275/00P).

References and Notes

(1) Mercer, R. S.; Harrison, A. G. *Can. J. Chem.* **1988**, *66*, 2947.

(2) Raftery, M. J.; Bowie, J. H.; Sheldon, J. C. *J. Chem. Soc., Perkin Trans. 2* **1988**, 563.

(3) Eichinger, P. C. H.; Bowie, J. H. *J. Chem. Soc., Perkin Trans. 2* **1988**, 497.

(4) Eichinger, P. C. H.; Bowie, J. H.; Blumenthal, T. *J. Org. Chem.* **1986**, *51*, 5078.

(5) Sheldon, J. C.; Bowie, J. H.; Lewis, D. E. *New. J. Chem.* **1988**, *12*, 269.

(6) Tumas, W.; Foster, R. F.; Pellerite, M. J.; Brauman, J. I. *J. Am. Chem. Soc.* **1984**, *106*, 4053.

(7) Tumas, W.; Foster, R. F.; Pellerite, M. J.; Brauman, J. I. *J. Am. Chem. Soc*. **1983**, *105*, 7464.

(8) Tumas, W.; Foster, R. F.; Brauman, J. I. *J. Am. Chem. Soc*. **1988**, *110*, 2714.

(9) Tumas, W.; Foster, R. F.; Pellerite, M. J.; Brauman, J. I. *J. Am. Chem. Soc*. **1987**, *109*, 961.

(10) Hayes, R. N.; Sheldon, J. C.; Bowie, J. H.; Lewis, D. E. *Aust. J. Chem*. **1985**, *38*, 1197.

(11) Hayes, R. N.; Sheldon, J. C.; Bowie, J. H.; Lewis, D. E. *J. Chem. Soc., Chem. Commun*. **1984**, 1431.

(12) Chiu, S.-W.; Lau, J. K.-C.; Li, W.-K. *J. Phys. Chem. A* **2001**, *105*, 432.

(13) Chiu, S.-W.; Lau, K.-C.; Li, W.-K. *J. Phys. Chem. A*. **1999**, *103*, 6003.

(14) Curtiss, L. A.; Raghavachari, K.; Redfern, P. C.; Redfern, V.; Pople, J. A. *J. Chem. Phys.* **1998**, *109*, 7764.

(15) Frisch, M. J.; Trucks, G. W.; Schlegel, H. B.; Gill, P. M. W.; Johnson, B. G.; Robb, M. A.; Cheeseman, J. R.; Keith, T.; Petersson, G. A.; Montgomery, J. A.; Raghavachari, K.; Al-Laham, M. A.; Zakrzewski, V. G.; Ortiz, J. V.; Foresman, J. B.; Cioslowski, J.; Stefanov, B. B.; Nanayakkara, A.; Challacombe, M.; Peng, C. Y.; Ayala, P. Y.; Chen, W.; Wong, M. W.; Andres, J. L.; Replogle, E. S.; Gomperts, R.; Martin, R. L.; Fox, D. J.; Binkley, J. S.; Defrees, D. J.; Baker, J.; Stewart, J. P.; Head-Gordon, M.; Gonzalez, C.; Pople, J. A. *Gaussian 94*, revision D.4; Gaussian, Inc.: Pittsburgh, PA, 1995.

(16) Frisch, M. J.; Trucks, G. W.; Schlegel, H. B.; Scuseria, G. E.; Robb, M. A.; Cheeseman, J. R.; Zakrzewski, V. G.; Montgomery, J. A., Jr.; Stratmann, R. E.; Burant, J. C.; Dapprich, S.; Millam, J. M.; Daniels, A. D.; Kudin, K. N.; Strain, M. C.; Farkas, O.; Tomasi, J.; Barone, V.; Cossi, M.; Cammi, R.; Mennucci, B.; Pomelli, C.; Adamo, C.; Clifford, S.; Ochterski, J.; Petersson, G. A.; Ayala, P. Y.; Cui, Q.; Morokuma, K.; Malick, D. K.; Rabuck, A. D.; Raghavachari, K.; Foresman, J. B.; Cioslowski, J.; Ortiz, J. V.; Stefanov, B. B.; Liu, G.; Liashenko, A.; Piskorz, P.; Komaromi, I.; Gomperts, R.; Martin, R. L.; Fox, D. J.; Keith, T.; Al-Laham, M. A.; Peng, C. Y.; Nanayakkara, A.; Gonzalez, C.; Challacombe, M.; Gill, P. M. W.; Johnson, B. G.; Chen, W.; Wong, M. W.; Andres, J. L.; Head-Gordon, M.; Replogle, E. S.; Pople, J. A. *Gaussian 98*, revision A.7; Gaussian, Inc.: Pittsburgh, PA, 1998.

(17) Curtiss, L. A.; Redfern, P. C.; Raghavachari, K.; Rassolov, V.; Pople, J. A. *J. Chem. Phys.* **1999**, *110*, 4703.

(18) Lias, S. G.; Bartmess, J. E.; Liebman, J. F.; Holmes, J. L.; Levin, R. D.; Mallard, W. G. *J. Phys. Chem. Ref. Data* **1988**, *17* (Suppl.1).

(19) Chiu, S.-W.; Cheung, Y.-S.; Ma, N. L.; Li, W.-K.; Ng, C. Y. *J. Mol. Struct. (THEOCHEM)* **1998**, *452*, 97.

(20) Morton, T. H. *Org. Mass Spectrom.* **1992**, *27*, 353.

(21) *NIST Chemistry WebBook, NIST Standard Reference Database Number 69*; Mallard, W. G., Linstrom, P. J., Eds.; National Institute of Standards and Technology: Gaithersburg, MD, 1998; http://webbook.nist.gov.